IIETA International Information and Engineering Technology Association
Advancing the World of Information and Engineering

Annales de Chimie - Science des Matériaux
Vol. 48, No. 5, October, 2024, pp. 739-745
Journal homepage: http://iieta.org/journals/acsm

Effect of GGBFS on the Compressive Strength of Geopolymers Binders

Naaem M. Al-Hantoosh*, Harith Abdullah Ali, Sawsan Abdullah Hassan, Wisam Dheyab

Civil Engineering Department, College of Engineering, Tikrit University, Tikrit 34001, Iraq

Corresponding Author Email: hantooshnaaem@gmail.com

https://doi.org/10.18280/acsm.480515

Received: 2 March 2024
Revised: 9 September 2024
Accepted: 18 September 2024
Available online: 29 October 2024

Keywords:
GGBFS, compressive strength, ordinary Portland cement, SEM and XRD analysis, compressive strength

ABSTRACT

Ground granulated blast furnace slag (GGBFS) conventionally has been mixed with ordinary Portland cement (OPC) owing to decrease the ecological impact and improve the engineering behavior. Concrete with GGBFS illustrates different strength enhancement of normal concrete, but sensitive, to environmental situation. Recently, the studies of decreasing the environmental impact of utilizing ordinary Portland cement in concrete production showed great attention. In this range, this study highlights the using of local blast furnace slag in producing cementitious material. In this paper, alkali-activated GGBFS replaced the OPC and ordinary GGBFS by ratios calculated by several compressive experiments. Compressive strength demonstrated that CB40 and CB50 have equal compressive strength as OPC. On the contrary, ACB60 showed (36%) increase in compressive strength over OPC for (28 days) curing. SEM and XRD analysis demonstrated formation of high content gels by incorporation alkali agent.

1. INTRODUCTION

Concrete is one of the most common materials consumed in construction due to its many benefits. The high cement consumption has caused an increasing of the global warming [1]. Production of OPC is one of the dominant sources for dioxide carbon emissions [2]. The cement industries consume approximately (12-15%) of the total energy consumption which used in all industries throughout the world [3, 4]. The High energy consumption is also increasing Carbon dioxide emission due to the increasing the use of cement in construct infrastructure and buildings for a higher population prompted researchers to find new ecologically friendly alternatives to cement [5-7].

Alkali activated material (AAM) (binder material) is one of the future cement replacement which appear to likeness a mechanical properties of Portland cement [8], in spite of the likeness in the mechanical properties as Portland cement, nevertheless is too early to use as replacement. AAM can be produced by adding powder form of an aluminosilicate – cab be obtained by product of other industrial or other low cost materials- with concentrated aqueous solution to be alkaline activator. Alkaline activator is usually used alkali hydroxide, silicate, carbonate or sulfate. Shi et al. [6] categorized five types for alkali-activated cement materials: Alkali-activated pozzolan cements, alkali-activated lime-pozzolan/slag cement, alkali-activated Portland blended cement (hybrid cements), alkali-activated slag-based cements, and alkali-activated calcium aluminate blended cement.

Alkali-activated cements formerly used Metakaolin, fly ash, and slag [9]. In steel production during iron formation, molten blast furnace slag quickly cools and forms glass granules [10]. POFA was mixed with rice husk ash (RHA), GGBFS, and fly ash as alomino-silicate ingredients to make geopolymer concrete [11, 12]. Kuhl introduced alkali activation in 1908, and Davidovits termed it geopolymer [13]. Poly-intensification of hydrolyzed aluminate and silicate caused the geopolymer binder's zeolitic crystalline structure [14]. In previous studies, geopolymeric gel and calcium silicate hydrate were also found together. Calcium silicate hydrate (C-S-H) was mostly generated by dissolving calcium in alkali with accessible silicates [15]. Synchronized geopolymeric gel and Calcium silicate hydrate (C-S-H) production may help fill binder voids and increase concrete's initial compressive strength. Dosage and kind of alkali activators determine gel formation and characteristics [16]. Sodium silicate (water glass) and sodium hydroxide (NaOH) were the most used geopolymer activating solutions [17].

According to Komnitsas and Zaharaki, alkali hydroxide dissolves aluminum-silicate sources, whereas sodium silicate solution works as a paste, activator, and plasticizer [18]. However, silicate solution is favored activating solution since it is available in liquid water glasses and increases polymerization reaction ratio [19]. Alkaline solutions induce enough Silicon and Aluminum atoms to form polymer particles, which poly-condense to create a solid [20]. Geopolymer binder characteristics are greatly affected by S/L and SS/SH ratios [21, 22]. To activate fly ash for geopolymerization, the solid-to-liquid mass ratio should be 3.0 [23]. However, particle form affects alkali activator mass needed for disintegration. Fly ash is better than Metakaolin for alkali activation because its spherical particle shape reduces the required liquid. Metakaolin's flaky shape increases the liquid demand. S/L (0.8) by mass is recommended for Metakaolin activation with optimal strength [24, 25]. Few studies examined Na2SiO3-NaOH ratio. The compressive strength of geopolymer concrete with low-calcium fly ash depended on the alkaline activator ratio. Their investigation

found that increasing the sodium silicate to sodium hydroxide (SS/SH) ratio increased geopolymer concrete compressive strength by 28% [26]. A 2.5 mass ratio was advised, whereas Wang et al. reported 0.24 for geopolymer-based Metakaolin [27].

Ground Granular blast slag can be water-cooled to make ground granular blast slag. Slow air-quenching produces inactive crystalline combinations in BF. One ton of steel produces 300 kg of GGBFS [28, 29]. GGBFS concrete combinations reduce hydration heat, enhance concrete strength and durability, and are environmentally friendly [30]. Engineering construction often substitutes OPC with GGBFS [31, 32]. (GGBFS) has been combined OPC to reduce ecological burden and improve concrete engineering properties [33]. However, GGBFS is sensitive to curing circumstances and weak in early ages [34, 35]. Many studies have examined cement hydration to determine GGBFS behavior in concrete [12, 36]. Morrow III et al. [37] examined CO_2 emissions and energy efficiency against cost analysis. Kim [16] found that high-volume GGBFS replacement up to 70% improved concrete durability and sustainability. GGBFS concrete has numerous advantages, including durability and long-term strength [38, 39], although it has poor initial strength and high shrinkage. Many research demonstrated that adding alkaline solution increases early strength, and others offered formulas for GGBFS slag concrete shrinkage [40, 15].

It must also anticipate GGBFS concrete's compressive strength, elastic modulus, creep, splitting tensile strength, and shrinkage. The combined effect of GGFBS slag and ultrafine palm oil fuel ash on geopolymer binder microstructure and compressive strength was studied [41]. Islam et al. [42] examined GGBFS and POFA geopolymeric binder mechanical characteristics. The binary mixture with low POFA and GGBS had the maximum compressive strength geopolymer binder. Previous research did not examine geopolymer activation and microstructure from POFA activation as an aluminosilicate material source [43]. This study promotes GGBFS as an eco-friendly cementitious material in concrete and other construction projects.

The study objectives include investigating of the process GGBFS and NaOH generate geopolymer binder, and the ratio of GGBFS to OPC and sodium hydroxide to water will be studied. These findings will also illuminate geopolymer binder's process and microstructure. This study may encourage further research on GGBFS geopolymer mortar and concrete behavior, as well as make concrete more environmentally friendly by reducing energy use and CO_2 emissions. This study examined hardened geopolymer binders' mechanical characteristics, microstructure, and oxides using SEM-EDS and XRD.

2. EXPERIMENTAL METHODS

2.1 Materials

2.1.1 Cementitious materials

Two types of binder materials were used in this study ordinary Portland cement OPC and Ground granular blast furnace slag. GGFBS was used in this study had fineness of 4485 cm^2/gm and density 2.94 g/cm^3. GGBFS was according to ASTM C 989-18 [44]. OPC was accordance with ASTM C150 [45]. Chemical composition of GGBFS and OPC were determined by (XRF) test X-Ray Fluorescence. All main chemical composition and physical properties were showed in Table 1.

Table 1. Physical properties and chemical compositions of OPC and GGBFS

Sample	Surface area (cm^2/g)	Density (g/cm^3)	Ig.loss (%)*	Chemical Compositions							
				SiO_2	CaO	Al_2O_3	Fe_2O_3	MgO	SO_3	MnO	TiO_2
OPC	3518	3.15	1.2	21.78	63.53	5.37	3.26	1.67	2.47		
GGBFS	4345	2.92	0.35	34.36	44.31	14.34	0.62	4.24	0.34	0.24	0.74

*Ignition Loss from 110℃ to 1000℃

2.1.2 Alkaline activator (AA)

Sodium hydroxide was used as alkali activators in this study. The purity of used sodium hydroxide was 99% with a concentration of 10 M. Then, NaOH powder was added to solution by mixing powder with water and left for one day to decrease the temperature of reaction before using in casting of samples in this study.

2.1.3 Fine aggregate (FA)

The fine aggregate was used in this investigation was sand with graded distribution in accordance to ASTM C778 [46] as shown in Table 2. Sand had specific gravity of 2.45 g/cm^3 and fineness modulus 2.01.

2.2 Mix proportions and mixing procedure

The experimental work in this research was conducted three main steps of works study. In step-1, preparing reference cement mortar by using traditional concrete materials (cement 557.2 kg/m^3, water-cement ratio 0.48, and sand/cement of 2.75with respect to ASTM C109 [47]. In Step-II, the main step focused on studying the properties of cement mortar after replacing OPC by GGBFS and selects the suitable percent of GGBFS. Step-III concentrated on additional enhancing of replacing mix water by alkali activator sodium hydroxide NaOH on the mortar of step-II, the mix proportions and mixing procedure of alkali activator sodium hydroxide NaOH according to [21]. In order to study the effect of addition of granular blast furnace slag and alkali activators, Sodium Hydroxide to cement mortar, seven different mortar mixtures (the mix proportions and mixing procedure of were presented he combined effect of GGFBS slag on geopolymer was studied [41]). Two types of cementitious materials OPC and GGBFS are used with three different cement replacement levels of 40%, 50%, and 60% were considered for GGBFS. Using Alkali activator as liquid Martials for mixing dry cement mortar with 40%,50%, and 60% OPC to GGBFS replacing ratio (see Table 3). mass of GGBFS was kept under to 20% In all mixes of present study mixtures to give satisfactory mechanical properties and workability [48]. Alkali Activator NaOH was prepared by adding water to dry powder 24 hours before casting the cement mortar. The mixing process included mixing different dry binder materials for 1 minutes after that adding water or AA (NaOH solution) and mixing for other 3*4 minutes for consistency and at last casting in mold for 7 and 28-days compressive strength.

Table 2. Sieve analysis of sand

Sieve Size (mm)	1.18 mm (No. 16)	600 µm (No. 30)	425 µm (No. 40)	300 µm (No. 50)	150 µm (No. 100)
ASTM C778	100	96-10	65-75	20-30	0-4
Passing Grade	100	98	72	26	3

Table 3. Proportion of mortar mixture

Mortar	Cement (Kg/m^3)	Liquid/binder	GGBFS/OPC	Water (L/m^3)	Sand (Kg/m^3)	GGBFS (Kg/m^3)	Alkaline (10M NaOH l/m^3)
OPC	557.2	0.48	-	267.46	1806	-	-
CB40	334.32	0.48	0.4	267.46	1806	222.88	-
CB50	278.6	0.48	0.5	267.46	1806	278.6	`-
CB60	222.88	0.48	0.6	267.46	1806	334.32	-
ACB40**	334.32	0.48	0.4	-	1806	222.88	267.46
ACB50	278.6	0.48	0.5	-	1806	278.6	267.46
ACB60	222.88	0.48	0.6	-	1806	334.32	267.46

*A (Alkaline activator), C (Portland Cement), B(GGBFS), 40(B/C Ratio)

3. RESULTS AND DISCUSSION

3.1 Compressive strength

Compressive strength of all samples were done in different ages 3, 7, and 28 days for (50*50*50mm) mortar cube according to ASTM C109 [47]. The GGBFS effect on the compressive strength of cement mortar can be showed in Table 4. Each value represents the average of three compressive strength test as a result. Increasing the alkali in the mixture ACB60 led to a decrease in the reaction water which reduced the hydration process of ordinary Portland cement OPC and thus led to a reduction in gel formation. Responsible for increasing the compressive resistance. Also, increasing the alkaline solution by GGBFS slag led to exceeding the optimum reaction ratio and a decrease in the required reaction ratio occurred, which led to a decrease in the compressive strength.

Table 4. Compressive strength

Sample	Compressive Strength (Mpa)		
	3 Days	7 Days	28 Days
OPC	32.08	38.48	40.91
CB40	31.10	37.63	40.34
CB50	30.68	36.57	39.70
CB60	25.52	30.61	33.57
ACB40	39.27	47.12	52.84
ACB50	42.03	52.34	56.03
ACB60	35.40	43.11	46.15

3.2 Mineralogy and microstructure

3.2.1 XRF test

The chemical compositions of all mortar types are determined by (XRF) test X-Ray Fluorescence (see Table 5).

3.2.2 XRD

Figure 1a and 1b present the XRD of sand-(50%)GGBFS-(50%)cement and sand-(60%)GGBFS-(40%)cement mixtures treated with 10 M of NaOH after 28 days of curing. Peaks of quartz, brucite, kaolinite, serpentine, sodium silicate (Na_2SiO_3) and mullite are defined as a result of olivine dissolution through the sodium hydroxide in soil. Peaks of quartz (SiO_2) (9, 24, 26, 28, 39, and 45°), brucite (18, 21, 36, and 48°), and sodium silicate (30 and 35°) were detected throughout the patterns [48, 49]. The figure shows the XRD analysis of 20% olivine-treated soil after 12, 48, and 168 h of carbonation under 200 kPa. Increasing carbonation periods led to a decrease in the brucite and magnesium peaks, whereas nesquehonite peaks increased as result of the carbonation process.

3.2.3 SEM

Figure 2a shows the microstructure of sand cement mortar. Figure 2b presents sand-(40%)GGBFS-(60%)cement mixture. Figures 2c and 2d present sand-(50%)GGBFS-(50%)cement and sand-(60%)GGBFS-(40%)cement mixtures treated with 10 Molarity of NaOH after 28 days of curing. Figure 2a demonstrates that the morphology of sand cement mortar consists of groups of connected particles, whereas the clustery particles seems more connected for sand mixed with (40%) GGBFS and (60%) cement in Figure 2b. Figure 2c clarifies the sand-cement-GGBFS treated mixture after curing. By making a comparison of Figures 2a and 2b with Figures 2c and 2d, it shows how alkali-activated treatment gives a more dens mass, and fills the voids of the sand with gel as a result of GGBFS decomposition and precipitation. Thus, SEM images reveal a dens morphology with few or no gaps, which is stable with the mechanical properties illustrated. Figures 2c and 2d evidence the existence of a new amorphous phase, which show the formation of a gels material surrounding sand particles.

Table 5. Chemical composition of mortar by XRF test

Sample	SiO_2	CaO	Al_2O_3	Fe_2O_3	MgO	SO_3	MnO	TiO_2	K_2O
OPC	34.38	30.38	2.906	3.08	1.646	1.073	0.095	0.285	0.438
CB40	47.01	18.27	1.938	3.564	0.849	5.329	0.248	0.206	0.443
CB50	44.02	18.11	2.113	4.194	1.003	5.965	0.299	0.221	0.373
CB60	40.07	20.20	2.245	4.741	1.073	6.542	0.354	0.204	0.3624
ACB40	24.74	21.14	1.991	3.371	1.151	6.138	0.240	0.2003	4.404
ACB50	34.93	20.79	2.138	4.737	1.024	5.530	0.355	0.201	4.804
ACB60	32.34	18.73	2.1	4.411	1.084	5.629	0.331	0.225	6.51

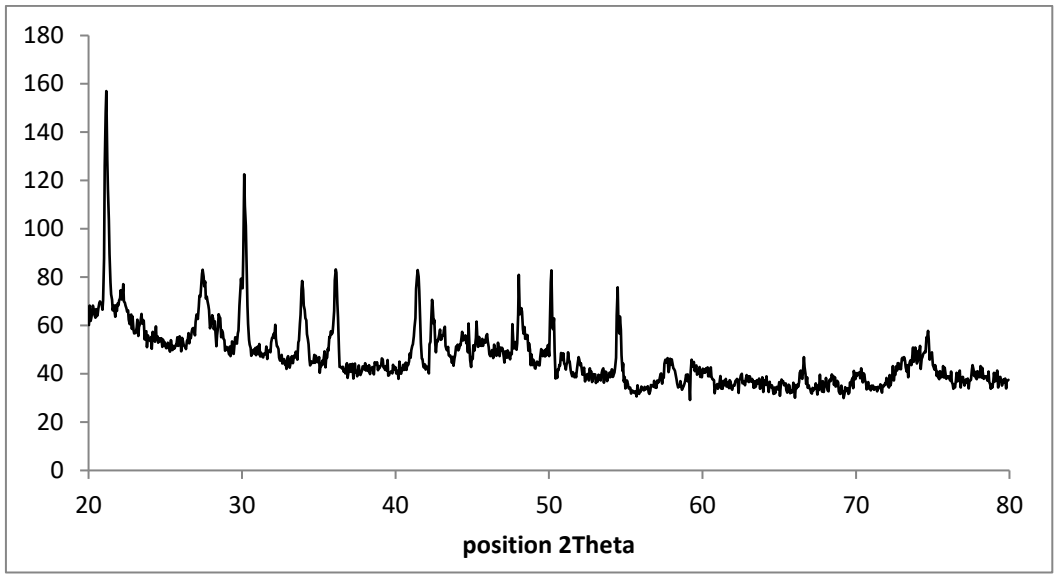

(a)

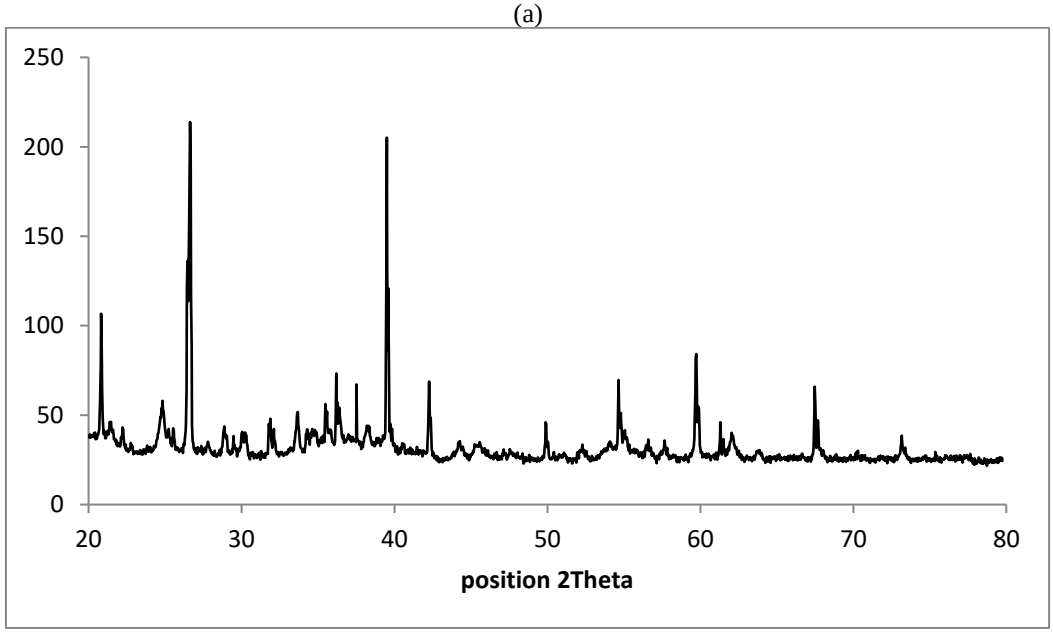

(b)

Figure 1. XRD of (a) ACB50; (b) ACB60

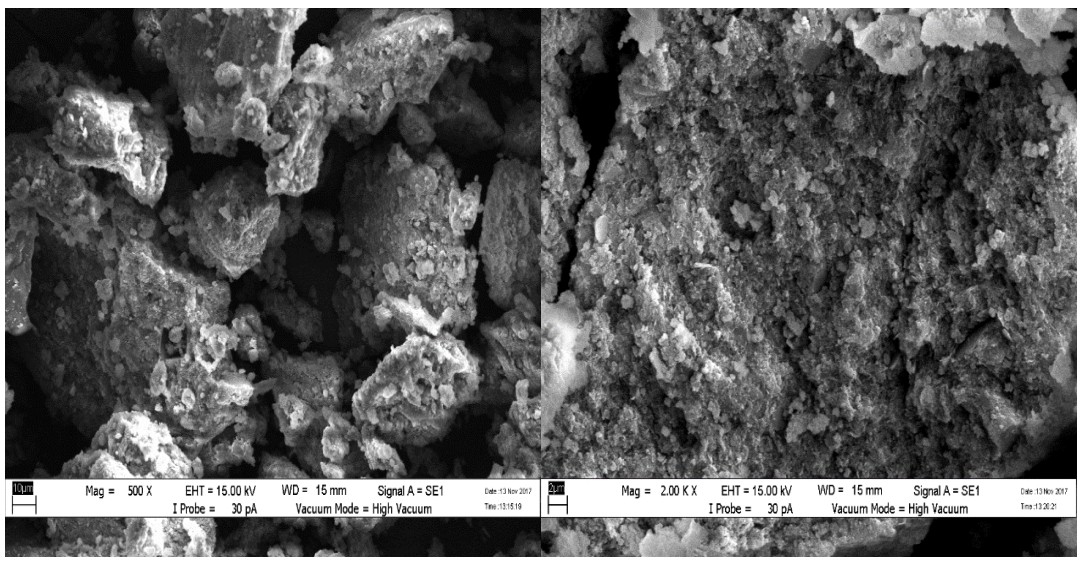

(a) (b)

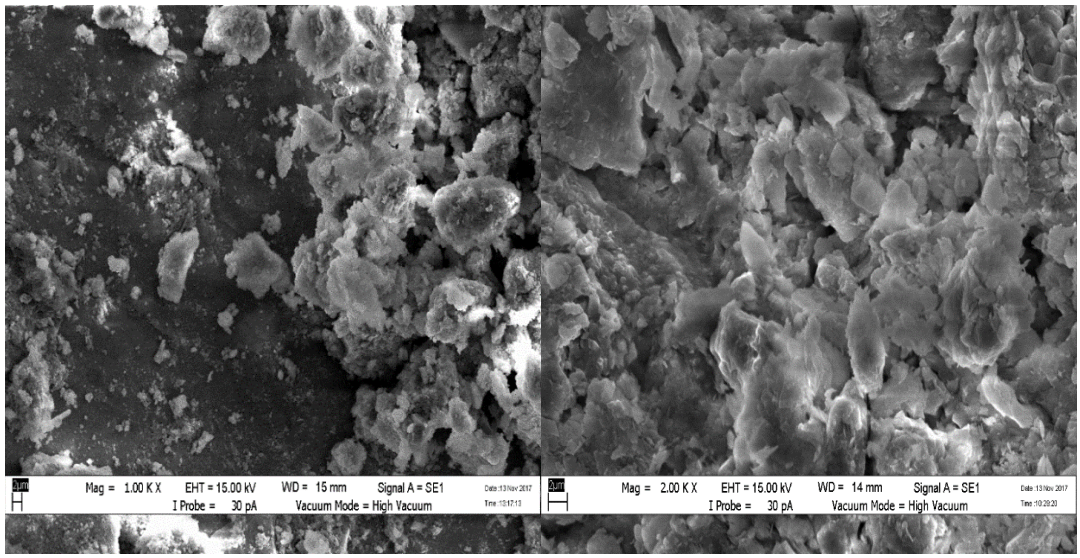

(c) (d)

Figure 2. SEM images of (a) OPC (b) CB40 (c) ACB50 (d) ACB60

4. CONCLUSIONS

The compressive strength test results of OPC, CB40, CB50, CB60, ACB50, and ACB60 slag concretes and alkali-activated slag concretes were assessed to test the probability of using GGBFS slag as a cementitious material. Based on the previous results, the following conclusions can be made:

1. The properties of fresh concrete were examined by measuring the compressive strength and the particle morphology were examined by XRD and SEM analysis. The cement content in the mixtures were substituted by GGBFS. Compressive strength tests showed that CB40 and CB50 reflected the highest compressive strength in (28 days).
2. Selected GGBFS contents (CB40, CB50 and CB60) were alkali-activated. Compressive tests of (ACB50 and ACB60) demonstrated an increase in compressive strength with time.
3. SEM and XRD of ACB50 and ACB60 showed increase in gel content with activation time increase. As a consequence, compressive strength of ACB50 and ACB60 showed highest values.
4. Based on SEM and XRD results analysis, we could confirm the reaction characteristics of ground granulated blast furnace slag. Major reaction products were found to be calcium silicate hydrate gel and Ca $(OH)_2$.
5. The researcher suggests for future work to study the effect of high temperatures on the mixtures that were used in the current study.

REFERENCES

[1] Shen, W., Liu, Y., Yan, B., Wang, J., He, P., Zhou, C., Huo, X., Zhang, W., Xu, G., (2017). Cement industry of China: Driving force, environment impact and sustainable development. Renewable and Sustainable Energy Reviews, 75: 618-628. https://doi.org/10.1016/j.rser.2016.11.033

[2] Miller, S.A., Horvath, A., Monteiro, P.J. (2016). Readily implementable techniques can cut annual CO_2 emissions from the production of concrete by over 20%. Environmental Research Letters, 11(7): 074029. https://doi.org/10.1088/1748-9326/11/7/074029

[3] Verma, Y., Mazumdar, B., Ghosh, P. (2020). Dataset on the electrical energy consumption and its conservation in the cement manufacturing industry. Data in Brief, 28: 104967. https://doi.org/10.1016/j.dib.2019.104967

[4] Ali, M.B., Saidur, R., Hossain, M.S. (2011). A review on emission analysis in cement industries. Renewable and Sustainable Energy Reviews, 15(5): 2252-2261. https://doi.org/10.1016/j.rser.2011.02.014

[5] Shekhovtsova, J., Zhernovsky, I., Kovtun, M., Kozhukhova, N., Zhernovskaya, I., Kearsley, E. (2018). Estimation of fly ash reactivity for use in alkali-activated cements-A step towards sustainable building material and waste utilization. Journal of Cleaner Production, 178: 22-33. https://doi.org/10.1016/j.jclepro.2017.12.270

[6] Shi, C., Shi, Z., Hu, X., Zhao, R., Chong, L. (2015). A review on alkali-aggregate reactions in alkali-activated mortars/concretes made with alkali-reactive aggregates. Materials and Structures, 48: 621-628. https://doi.org/10.1617/s11527-014-0505-2

[7] Vishwakarma, V., Ramachandran, D. (2018). Green concrete mix using solid waste and nanoparticles as alternatives–A review. Construction and Building Materials, 162: 96-103. https://doi.org/10.1016/j.conbuildmat.2017.11.174

[8] Karim, M.R., Hossain, M.M., Elahi, M.M.A., Zain, M.F.M. (2020). Effects of source materials, fineness and curing methods on the strength development of alkali-activated binder. Journal of Building Engineering, 29: 101147. https://doi.org/10.1016/j.jobe.2019.101147

[9] Abdalqader, A., Jin, F., Al-Tabbaa, A. (2019). Performance of magnesia-modified sodium carbonate-activated slag/fly ash concrete. Cement and Concrete Composites, 103: 160-174. https://doi.org/10.1016/j.cemconcomp.2019.05.007

[10] Aziz, I.H., Abdullah, M.M.A.B., Salleh, M.M., Azimi, E.A., Chaiprapa, J., Sandu, A.V. (2020). Strength development of solely ground granulated blast furnace slag geopolymers. Construction and Building Materials,

250: 118720. https://doi.org/10.1016/j.conbuildmat.2020.118720
[11] Al Safi, A.A. (2019). Blast furnace slag-based geopolymer mortars cured at different conditions: Modeling and optimization of compressive strength. European Journal of Environmental and Civil Engineering, 25(11): 1949-1962. https://doi.org/10.1080/19648189.2019.1598502
[12] Kim, D., Kim, C.Y., Urgessa, G., Choi, J.H., Park, C., Yeon, J.H. (2019). Durability and rheological characteristics of high-volume ground-granulated blast-furnace slag concrete containing $CaCO_3$/anhydrate-based alkali activator. Construction and Building Materials, 204: 10-19. https://doi.org/10.1016/j.conbuildmat.2019.01.141
[13] Finocchiaro, C., Barone, G., Mazzoleni, P., Leonelli, C., Gharzouni, A., Rossignol, S. (2020). FT-IR study of early stages of alkali activated materials based on pyroclastic deposits (Mt. Etna, Sicily, Italy) using two different alkaline solutions. Construction and Building Materials, 262: 120095. https://doi.org/10.1016/j.conbuildmat.2020.120095
[14] Rashidian-Dezfouli, H., Rangaraju, P.R., Kothala, V.S.K. (2018). Influence of selected parameters on compressive strength of geopolymer produced from ground glass fiber. Construction and Building Materials, 162: 393-405. https://doi.org/10.1016/j.conbuildmat.2017.09.166
[15] Kubba, Z., Huseien, G.F., Sam, A.R.M., Shah, K.W., Asaad, M.A., Ismail, M., Tahir, M.M., Mirza, J. (2018). Impact of curing temperatures and alkaline activators on compressive strength and porosity of ternary blended geopolymer mortars. Case Studies in Construction Materials, 9: e00205. https://doi.org/10.1016/j.cscm.2018.e00205
[16] Kim, T. (2019). The effects of polyaluminum chloride on the mechanical and microstructural properties of alkali-activated slag cement paste. Cement and Concrete Composites, 96: 46-54. https://doi.org/10.1016/j.cemconcomp.2018.11.010
[17] Abbas, R., Khereby, M.A., Ghorab, H.Y., Elkhoshkhany, N. (2020). Preparation of geopolymer concrete using Egyptian kaolin clay and the study of its environmental effects and economic cost. Clean Technologies and Environmental Policy, 22: 669-687. https://doi.org/10.1007/s10098-020-01811-4
[18] Aziz, I.H., Al Bakri Abdullah, M.M., Yong, H.C., Ming, L.Y., Hussin, K., Surleva, A., Azimi, E.A. (2019). Manufacturing parameters influencing fire resistance of geopolymers: A review. Proceedings of the Institution of Mechanical Engineers, Part L: Journal of Materials: Design and Applications, 233(4): 721-733. https://doi.org/10.1177/1464420716668203
[19] Luukkonen, T., Sreenivasan, H., Abdollahnejad, Z., Yliniemi, J., Kantola, A., Telkki, V.V., Kinnunen, P., Illikainen, M. (2020). Influence of sodium silicate powder silica modulus for mechanical and chemical properties of dry-mix alkali-activated slag mortar. Construction and Building Materials, 233: 117354. https://doi.org/10.1016/j.conbuildmat.2019.117354
[20] Kuenzel, C., Ranjbar, N. (2019). Dissolution mechanism of fly ash to quantify the reactive aluminosilicates in geopolymerisation. Resources, Conservation and Recycling, 150: 104421. https://doi.org/10.1016/j.resconrec.2019.104421
[21] Vu, C.M., Le, T.A., Satomi, T., Takahashi, H. (2017). Study on effect of chemical composition of geopolymer to improve sludge by using fiber materials. Advanced Experimental Mechanics, 2: 168-173. https://doi.org/10.11395/aem.2.0_168
[22] Wang, W., Noguchi, T. (2020). Alkali-silica reaction (ASR) in the alkali-activated cement (AAC) system: A state-of-the-art review. Construction and Building Materials, 252: 119105. https://doi.org/10.1016/j.conbuildmat.2020.119105
[23] Wang, Y., Liu, X., Zhang, W., Li, Z., Zhang, Y., Li, Y., Ren, Y. (2020). Effects of Si/Al ratio on the efflorescence and properties of fly ash based geopolymer. Journal of Cleaner Production, 244: 118852. https://doi.org/10.1016/j.jclepro.2019.118852
[24] Ohno, M. (2017). Green and durable geopolymer composites for sustainable civil infrastructure. Doctoral dissertation.
[25] Mohseni, E., Kazemi, M.J., Koushkbaghi, M., Zehtab, B., Behforouz, B. (2019). Evaluation of mechanical and durability properties of fiber-reinforced lightweight geopolymer composites based on rice husk ash and nano-alumina. Construction and Building Materials, 209: 532-540. https://doi.org/10.1016/j.conbuildmat.2019.03.067
[26] Jiao, Z., Wang, Y., Zheng, W., Huang, W. (2018). Effect of dosage of sodium carbonate on the strength and drying shrinkage of sodium hydroxide based alkali-activated slag paste. Construction and Building Materials, 179: 11-24. https://doi.org/10.1016/j.conbuildmat.2018.05.194
[27] Kohout, J., Koutník, P. (2020). Effect of filler type on the thermo-mechanical properties of metakaolinite-based geopolymer composites. Materials, 13(10): 2395. https://doi.org/10.3390/ma13102395
[28] Horii, K., Tsutsumi, N., Kato, T., Kitano, Y., Sugahara, K. (2015). Overview of iron/steel slag application and development of new utilization technologies. Nippon Steel & Sumitomo Metal Technical Report, 109: 5-11.
[29] Mombelli, D., Mapelli, C., Gruttadauria, A., Baldizzone, C., Magni, F., Levrangi, P.L., Simone, P. (2012). Analisys of electric arc furnace slag. Steel Research International, 83(11): 1012-1019. https://doi.org/10.1002/srin.201100259
[30] Wang, G.C. (2016). The Utilization of Slag in Civil Infrastructure Construction. Woodhead Publishing.
[31] ACI Committee 233. (2017). Guide to the Use of Slag Cement in Concrete and Mortar. ACI 223 American Concrete Institute: Farmington Hills, MI, USA.
[32] Pacewska, B., Wilińska, I. (2020). Usage of supplementary cementitious materials: Advantages and limitations: Part I. C–S–H, C–A–S–H and other products formed in different binding mixtures. Journal of Thermal Analysis and Calorimetry, 142(1): 371-393. https://doi.org/10.1007/s10973-020-09907-1
[33] Yang, H.M., Kwon, S.J., Myung, N.V., Singh, J.K., Lee, H.S., Mandal, S. (2020). Evaluation of strength development in concrete with ground granulated blast furnace slag using apparent activation energy. Materials, 13(2): 442. https://doi.org/10.3390/ma13020442
[34] Korde, C., Cruickshank, M., West, R.P., Pellegrino, C. (2019). Activated slag as partial replacement of cement mortars: Effect of temperature and a novel admixture. Construction and Building Materials, 216: 506-524. https://doi.org/10.1016/j.conbuildmat.2019.04.172
[35] Soutsos, M., Hatzitheodorou, A., Kwasny, J., Kanavaris,

F. (2016). Effect of in situ temperature on the early age strength development of concretes with supplementary cementitious materials. Construction and Building Materials, 103: 105-116. https://doi.org/10.1016/j.conbuildmat.2015.11.034
[36] Mehta, P.K., Monteiro, P. (2014). Concrete: Microstructure, Properties, and Materials (4th ed.). McGraw-Hill Education: New York, NY, USA.
[37] Morrow III, W.R., Hasanbeigi, A., Sathaye, J., Xu, T. (2014). Assessment of energy efficiency improvement and CO_2 emission reduction potentials in India's cement and iron & steel industries. Journal of Cleaner Production, 65: 131-141. https://doi.org/10.1016/j.jclepro.2013.07.022
[38] Bostancı, Ş.C., Limbachiya, M., Kew, H. (2016). Portland slag and composites cement concretes: Engineering and durability properties. Journal of Cleaner Production, 112: 542-552. https://doi.org/10.1016/j.jclepro.2015.08.070
[39] Harbulakova, V.O., Estokova, A., Kovalcikova, M. (2017). Sustainable usage of slag in concrete for higher resistance in aggressive environment-mathematical evaluation. Chemical Engineering Transactions, 57: 481-486. https://doi.org/10.3303/CET1757081
[40] Yoo, D.Y., Park, J.J., Kim, S.W., Yoon, Y.S. (2013). Early age setting, shrinkage and tensile characteristics of ultra-high performance fiber reinforced concrete. Construction and Building Materials, 41: 427-438. https://doi.org/10.1016/j.conbuildmat.2012.12.015
[41] Ameri, F., Shoaei, P., Zareei, S.A., Behforouz, B. (2019). Geopolymers vs. alkali-activated materials (AAMs): A comparative study on durability, microstructure, and resistance to elevated temperatures of lightweight mortars. Construction and Building Materials, 222: 49-63. https://doi.org/10.1016/j.conbuildmat.2019.06.079
[42] Islam, A., Alengaram, U.J., Jumaat, M.Z., Bashar, I.I. (2014). The development of compressive strength of ground granulated blast furnace slag-palm oil fuel ash-fly ash based geopolymer mortar. Materials & Design, 56: 833-841. https://doi.org/10.1016/j.matdes.2013.11.080
[43] Al-Rkaby, A.H.J. (2019). Evaluating shear strength of sand-GGBFS based geopolymer composite material. Acta Polytechnica, 59(4): 305-311. https://doi.org/10.14311/AP.2019.59.0305
[44] ASTM C 989-18a. (2018). Standard Specification for Slag Cement for Use in Concrete and Mortars. ASTM International: West Conshohocken, PA, USA. https://doi.org/10.1520/C0989_C0989M-18A
[45] ASTM C150/C150M-18. (2018). Standard Specification for Portland Cement. ASTM International: West Conshohocken, PA, USA. https://doi.org/10.1520/C0150_C0150M-18
[46] ASTM C778-17. (2017). Standard Specification for Standard Sand. ASTM International: West Conshohocken, PA, USA. https://doi.org/10.1520/C0778-17
[47] ASTM C109/C109M-16a. (2016). Standard Test Method for Compressive Strength of Hydraulic Cement Mortars (Using 2-in. or [50-mm] Cube Specimens). ASTM International: West Conshohocken, PA, USA. https://doi.org/10.1520/C0109_C0109M-16A
[48] Komljenović, M., Baščarević, Z., Bradić, V. (2010). Mechanical and microstructural properties of alkali-activated fly ash geopolymers. Journal of Hazardous Materials, 181(1-3): 35-42. https://doi.org/10.1016/j.jhazmat.2010.04.064
[49] Yi, S.T., Noh, J.H., Kim, J.H., Lee, K.J. (2013). A study on the improvement of early-age compressive strength of smart BFS powder added cement mortar. Journal of the Korea Institute for Structural Maintenance and Inspection, 17(2): 135-141. https://doi.org/10.11112/jksmi.2013.17.2.135